MODEL PREDICTIVE CURRENT CONTROL OFGRID-CONNECTED THREE-PHASE INVERTER FOR PV SYSTEMS

ĐIỀU KHIỂN DÒNG ĐIỆN DỰ BÁO MÔ HÌNH CỦA BỘ NGHỊCH LƯU BA PHA NỐI LƯỚI CHO CÁC HỆ THỐNG QUANG ĐIỆN

Nguyen Thanh Son[1,*], Pham Hung Phi[1], Nguyen The Cong[1]
Le Anh Tuan[2], Pham Van Tuan[3]

ABSTRACT

This paper presents model predictive current control of a grid-connected two-level voltage-source three-phase inverter for a photovoltaic(PV) system. The output of a solar array is fed to a DC-DC boost converter to make a DC link voltage that is fed to theinverter. In this PVsystem, the theory of model predictive control (MPC) is applied to design an effective controller for the grid-connected currents. In addition, asuitable PI controller is used to compute the reference grid-connected currents and keep a DC link voltagefor the inverter to be constant. Model of the system is established to predict the controlled variables. Optimal switching states are selected by minimizing a cost function defined using the difference between the reference and measured grid-connected currents for each sampling period. Simulation results obtained using MATLAB/Simulink show that if the reference currents change dynamically, the model predictive controller has the ability of fast current regulation. Moreover, thiscontroller can also result in an effectively injectionof the active power into the grid.

Keywords: *There-phase inverter, grid-connected, model predictive control, PV systems.*

TÓM TẮT

Bài báo này trình bày điều khiển dòng điện dự báo mô hình cho một bộ nghịch lưu ba pha nguồn áp hai mức nối lưới trong một hệ thống quang điện. Đầu ra của mảng pin mặt trời được cấp cho đầu vào của một bộ biến đổi DC-DC tăng áp để tạo một điện áp một chiều cấp cho đầu vào của bộ nghịch lưu. Đối với hệ thống quang điện này, lý thuyết điều khiển dự báo mô hình được áp dụng để thiết kế một bộ điều khiển dòng điện nối lưới hiệu quả. Thêm vào đó, một bộ điều khiển P-I phù hợp được sử dụng để tính toán dòng điện nối lưới tham chiếu. Mô hình của hệ thống được thiết lập để dự báo các biến được điều khiển. Các trạng thái chuyển mạch tối ưu được chọn bằng cách cực tiểu hóa một hàm chi phí dựa trên sai lệch giữa dòng điện nối lưới tham chiếu và dòng điện nối lưới thực đo được trong mỗi chu kỳ lấy mẫu. Kết quả mô phỏng thu được bằng Matlab/Simulink cho thấy rằng nếu dòng điện nối lưới tham chiếu thay đổi, bộ điều khiển dự báo mô hình có khả năng điều chỉnh dòng điện nhanh. Hơn nữa, bộ điều khiển nàycó thể tạo nên quá trình phát công suất tác dụng vào lưới hiệu quả.

Từ khóa: *Nghịch lưu ba pha, nối lưới, điều khiển dự báo mô hình, hệ thống quang điện.*

[1]School of Electrical Engineering, Hanoi University of Science and Technology
[2]Faculty of Electrical Engineering, Hanoi University of Industry
[3]Faculty of Electrical Engineering, Vinh University of Technology Education
[*]Email: son.nguyenthanh@hust.edu.vn
Received: 15/01/2021
Revised: 20/3/2021
Accepted: 25/4/2021

1. INTRODUCTION

The lack of fossil energy and the increase of environmental pollution has significantly promoted the wide use of renewable energy. One of the most popular renewable energy sources is photovoltaic (PV) systems that can be used due to advances in technology and low prices of solar panels. In PV systems, solar panels are connected generate a DC voltage that is not regulated or not at a proper level for power conversion. Then, such uncontrolled and unregulated DC voltage is regulated depending on specific load requirements. A DC-DC boost converter can be used for this purpose. The converter output voltage is sometimes DC link voltage and can be assumed as a voltage source. There are many Maximum Power Point Tracking (MPPT) control techniques used to extract maximum power from PV array in which Perturb and Observe (P&O) algorithm is most widely used due to its ease of implementation [1].

The majority of renewable energy systems (RESs) are used as grid-connected power sources due to the advantages of these systems and their role in emerging technical topics of modern power electronics such as micro-grids or smart-grids. Grid connection of RESs faces some challenges as usual. In particular, the harmonic generation can be seen one of the damaging phenomena in power sources that are connected the electrical network. In addition, these harmonics can be also considered as the main cause of damage to sensitive equipment. According to the IEEE-1547 standard, total harmonic distortion (THD) of the injected current into a grid should be less than 5%. There are two reasons for harmonic generation. The first comes from the nature of the inverter such as pulse width modulation

(PWM) and switching, and the second reason relates to load and grid.

In recent years, MPC has attracted a lot of attention in power electronics due to it can handle system limitations including nonlinearity, multi-variability and various system constrains [2, 3, 4]. Different MPC methods have been developed for power electronic converters [5, 6, 7]. The well-known MPC method is Finite Control Set-Model Predictive Control (FCS-MPC) as it does not require any modulator and control signals can be applied to system directly. In this research, the grid-connected current at the output of the inverter is controlled using the FCS-MPC.

The rest of this paper is organized into the following sections: In Section 2, a PV system is briefly described. Section 3 presents the model of the grid-connected three-phase inverter in the αβ-frame. In Section 4, the MPC method for the grid-connected current is mentioned. Simulation results and discussions are presented in Section 5. Finally, Section 6 is the conclusion of this research.

2. PV SYSTEMS

A PV system consists of a number of PV panels connected in series or parallel to form a DC PV array. When a load is directly connected to the PV array, the operating point will rarely be at peak power. The impedance seen by the PV array derives the operating point of the PV array. Therefore, by varying the impedance seen by the PV array, the operating point can be moved towards the peak power point. Since the PV array is a DC device, a DC-DC converter such as a boost DC-DC converter needs to be used to transform the impedance of one circuit (source) to the other circuit (load) as shown in Figure 1. Changing the duty cycle D of the boost DC-DC converter results in an impedance change as seen by the PV array. At a particular impedance (or duty cycle D), the operating point will be at the peak power transfer point. MPPT implementation utilizes algorithms that frequently sample PV array voltages and currents, then adjusts the duty cycle D as needed. In P&O method, the controller adjusts the voltage by a small amount from the array and measure power. If the power increases, further adjustments in that direction are tried until power no longer increases. It is referred as a "hill climbing" method because it depends on the rise of the curve of power against voltage below the maximum power point.

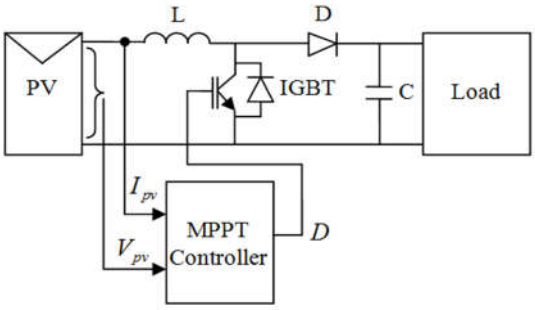

Figure 1. A DC PV system with MPPT using a DC-DC boost converter

3. MODEL OF THE GRID-CONNECTED THREE-PHASE INVERTER

The power circuit of a grid-connected three-phase inverter can be shown in Figure 2. V_{dc} is the DC link voltage, L is the filtering inductance and R is the line resistance. e_a is the grid voltage of phase A. i_a is the output current of phase A.

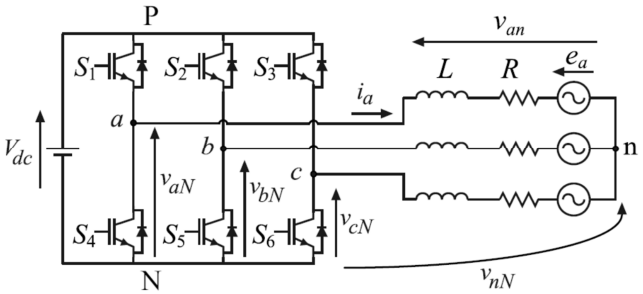

Figure 2. Power circuit of grid-connected three-phase inverter

In orderto describe the switching state of the inverter, the variables S_a, S_b and S_c are defined as:

$$S_a = \begin{cases} 1 & \text{if } S_1 \text{ on and } S_4 \text{ off} \\ 0 & \text{if } S_1 \text{ off and } S_4 \text{ on} \end{cases}$$

$$S_b = \begin{cases} 1 & \text{if } S_2 \text{ on and } S_5 \text{ off} \\ 0 & \text{if } S_2 \text{ off and } S_5 \text{ on} \end{cases}$$

$$S_c = \begin{cases} 1 & \text{if } S_3 \text{ on and } S_6 \text{ off} \\ 0 & \text{if } S_3 \text{ off and } S_6 \text{ on} \end{cases}$$

These switching signals define the values of the output voltage:

$$v_{aN} = S_a V_{dc} \quad (1)$$

$$v_{bN} = S_b V_{dc} \quad (2)$$

$$v_{cN} = S_c V_{dc} \quad (3)$$

where v_{aN}, v_{bN} and v_{cN} are the phase-to-neutral (N) voltages of the inverter. The switch state vector S is defined as:

$$S = \frac{2}{3}\left(S_a + aS_b + a^2 S_c\right) \quad (4)$$

where $a = e^{j2\pi/3} = -\frac{1}{2} + j\frac{\sqrt{3}}{2}$

The inverter output voltage vector *v* is defined as:

$$v = \frac{2}{3}\left(v_{aN} + av_{bN} + a^2 v_{cN}\right) \quad (5)$$

The relationship between the voltage vector v and the switch state vector S can be described as:

$$v = V_{dc} S \quad (6)$$

The possible combinations of the switching states generate the voltage vectors listed in Table 1, which can be represented in the complex plane as shown in Figure 3. The voltage vectors generated by the inverter are only seven different voltage vectors because V_0 and V_7 produce the

same zero voltage vector ($V_0 = V_7$). This means that a three-phase two-level voltage-source inverter can only generate 7 different voltage vectors.

Table 1. Switching states and the corresponding voltage vectors of the inverter

S_a	S_b	S_c	Voltage vector V
0	0	0	$V_0 = 0$
1	0	0	$V_1 = \frac{2}{3}V_{dc}$
1	1	0	$V_2 = \frac{1}{3}V_{dc} + j\frac{\sqrt{3}}{3}V_{dc}$
0	1	0	$V_3 = -\frac{1}{3}V_{dc} + j\frac{\sqrt{3}}{3}V_{dc}$
0	1	1	$V_4 = -\frac{2}{3}V_{dc}$
0	0	1	$V_5 = -\frac{1}{3}V_{dc} - j\frac{\sqrt{3}}{3}V_{dc}$
1	0	1	$V_6 = \frac{1}{3}V_{dc} - j\frac{\sqrt{3}}{3}V_{dc}$
1	1	1	$V_7 = 0$

For a balanced three-phase load, the current vector i and the grid voltage vector e can be expressed as:

$$i = \frac{2}{3}\left(i_a + ai_b + a^2 i_c\right) \quad (7)$$

$$e = \frac{2}{3}\left(e_a + ae_b + a^2 e_c\right) \quad (8)$$

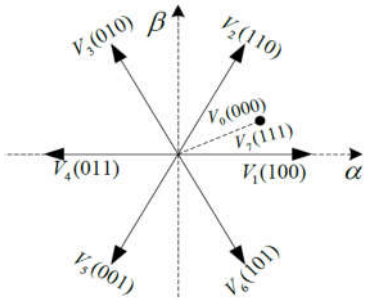

Figure 3. Voltage vectors of the three-phase inverter

The vector differential equation of the load current can be described as:

$$v = Ri + L\frac{di}{dt} + e \quad (9)$$

The Clark transform from the abc-frame to the αβ-frame has the following form:

$$\begin{bmatrix}\alpha\\ \beta\end{bmatrix} = \frac{2}{3}\begin{bmatrix}1 & -\frac{1}{2} & \frac{1}{2}\\ 0 & \frac{\sqrt{3}}{2} & -\frac{\sqrt{3}}{2}\end{bmatrix}\begin{bmatrix}a\\ b\\ c\end{bmatrix} \quad (10)$$

Equation (9) can be expressed in the αβ-frame as:

$$\begin{bmatrix}v_\alpha\\ v_\beta\end{bmatrix} = R\begin{bmatrix}i_\alpha\\ i_\beta\end{bmatrix} + L\frac{d}{dt}\begin{bmatrix}i_\alpha\\ i_\beta\end{bmatrix} + \begin{bmatrix}e_\alpha\\ e_\beta\end{bmatrix} \quad (11)$$

If the sampling time is defined as T_s, then:

$$\frac{d}{dt}\begin{bmatrix}i_\alpha\\ i_\beta\end{bmatrix} = \frac{1}{T_s}\begin{bmatrix}i_\alpha(k+1) - i_\alpha(k)\\ i_\beta(k+1) - i_\beta(k)\end{bmatrix} \quad (12)$$

From equation (11) and (12), we can obtain:

$$\begin{bmatrix}i_\alpha(k+1)\\ i_\beta(k+1)\end{bmatrix} = \frac{T_s}{L}\begin{bmatrix}v_\alpha(k) - e_\alpha(k)\\ v_\beta(k) - e_\beta(k)\end{bmatrix} + \left(1 - \frac{RT_s}{L}\right)\begin{bmatrix}i_\alpha(k)\\ i_\beta(k)\end{bmatrix} \quad (13)$$

where $i_\alpha(k)$ and $i_\beta(k)$ are the grid-connected currents at the k th sampling time in the αβ-frame coordinate. $v_\alpha(k)$ and $v_\beta(k)$ are the αβ-frame coordinate components of different voltage vectors at the kth sampling time. $e_\alpha(k)$ and $e_\beta(k)$ are the grid voltages at the kth sampling time in the αβ-frame coordinate. $i_\alpha(k+1)$ and $i_\beta(k+1)$ are the predicted grid-connected currents at the (k+1) th sampling time in the αβ-frame coordinate. Equation (13) can be seen as the predictive function of the grid-connected current.

4. MODEL PREDICTIVE CURRENT CONTROL STRATEGY

The main idea behind the model predictive current control strategy is to implement a discrete-time control scheme that selects the switching state that minimizes the predicted current error. The optimal switching state is applied during a whole sampling interval. This calculation is repeated during each sampling period using the measured currents *i* and reference values i^*. The measured currents and the predictive model are used in the calculation of the predicted currents $i^*(k+1)$, which are calculated for all possible switching states. Then the predicted currents are evaluated by using a cost function and the optimal switching state is selected as the one that minimizes this function. In this case, the cost function has the following form:

$$g = \left|i_\alpha^*(k+1) - i_\alpha(k+1)\right| + \left|i_\beta^*(k+1) - i_\beta(k+1)\right| \quad (14)$$

The model predictive current control structure of grid-connected three-phase inverter for a PV system is shown in Figure 4. The error between the reference DC link voltage V_{dc}(ref) and the actual DC link voltage V_{dc}(MPPT) determined from the MPPT technique is the input of a Proportional-Integral (PI) controller. The PI controller results in the appropriated amplitude of the reference current I^* and a nearly stable amplitude for the DC link voltage (the capacitor voltage). This phenomenon can be explained as follows: If the power generated by the PV array is greater than the power transmitted to the network, the additional generated power will be stored in the capacitor resulting in an increase of the capacitor voltage. If the power injected into the network by the inverter is greater than the power generated by the PV array, the capacitor voltage will decrease.

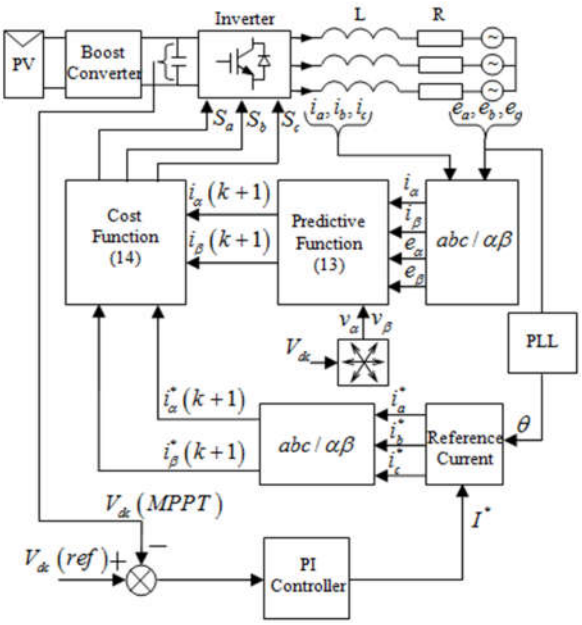

Figure 4. Model predictive current control structure of grid-connected three-phase inverter for a PV system

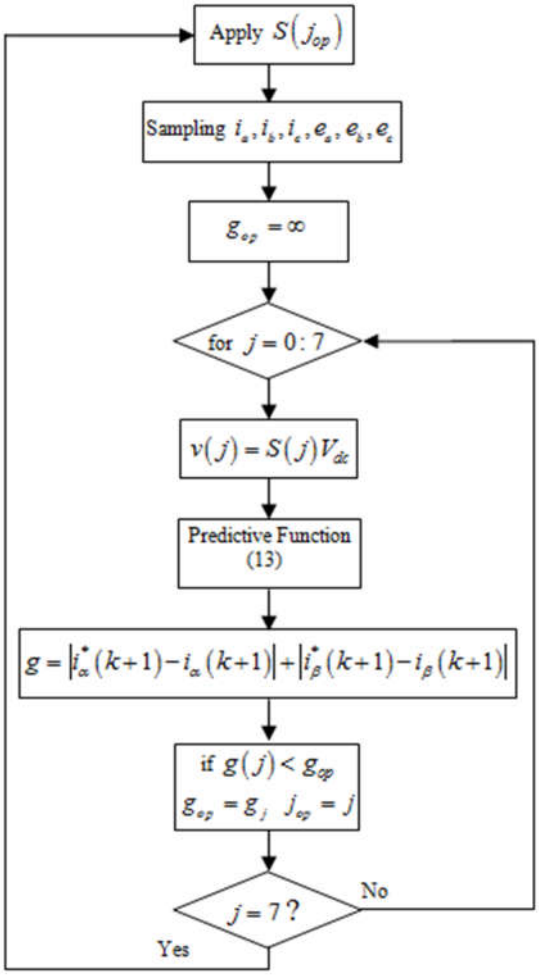

Figure 5. Flow chart of model predictive current control algorithm

Thus, it is required to select negative coefficients for PI controller. The angle θ is obtained by using a Phase Locked Loop (PLL). The combination of I^* and θ can be used to determine the reference three-phase currents i_a^*, i_b^*, i_c^*. Figure 5 shows the flow chart of model predictive current control algorithm.

5. SIMULATION RESULTS

Table 2 shows parameters of the commercial PV panel used in this research. MATLAB/Simulink software is used for simulation tasks. There are five branches of PV panels connected in parallel. For each branch, there are ten PV panels connected in series. Therefore, the maximum power of the PV system is approximately 6kW at the nominal operation condition. Table 3 shows parameters of the input of the inverter and the grid-connected three-phase load.

Table 2. Parameters of PV panel used for simulation

Parameters	Values
Nominal short-circuit voltage	$I_{scn} = 5.11$ (A)
Nominal array open-circuit voltage	$V_{ocn} = 29.80$ (V)
Panel current at maximum power point	$I_{pvn} = 4.74$ (A)
Panel voltage at maximum power point	$V_{mp} = 25.15$ (V)
Panel maximum output peak power	$P_{max\_e} = 120$ (W)
Voltage/temperature coefficient	$K_v = -0.38$ (V/K)
Current/temperature coefficient	$K_i = 0.04$ (A/K)
Series resistance	$R_s = 0.1683$ (Ω)
Parallel resistance	$R_p = 211.5173$ (Ω)
Nominal irradiance	$G_n = 1000$ (W/m^2)
Nominal operating temperature	$T_n = 25 + 273.15$ (K)
Boltzmann constant	k = 1.3806503e-23 (J/K)
Electron charge	q = 1.60217646e-19 (C)
Ideal diode factor	a = 1

Table 3. Parameters of the input of the inverter and the grid-connected three-phase load

Parameters	Values
Reference DC link voltage	$V_{dc\_ref} = 1000$ (V)
DC side voltage capacitor	C = 3000 (μF)
Filtering inductance	L = 10 (mH)
Line resistance	R = 0.01 (Ω)
Phase to phase grid voltage	e = 380 (V)

Figure 6 shows the DC link voltage stable at 1000(V).

The solar irradiation is assumed to change from 650(W/m^2) to 1000(W/m^2) at 0.1s corresponding to the ambient temperature of 25^{0}C as shown in Figure 7. The waveforms of the grid voltages and the grid-connected currents are shown in Figure 8 and Figure 9, respectively. Figure 10 is the output powers of the inverter. It is clear that the active power injected into the grid is nearly equal to the mmaximum output power extracted from the PV arrays. This means that the system has very high efficiency of power conversion and the reactive power is

approximatelyequal to zero. We can also see that the active power can change quickly according to the step change of the solar irradiation.

According to the harmonic analysis diagram in Figure 11, the grid-connected current has the THD of 2.85% corresponding to the solar irradiation of 650(W/m^2). When the solar irradiation rises up to 1000(W/m^2), the THD of the grid-connected current is only 1.76% as shown in Figure 12. In both cases, the THDs are less than 5%.

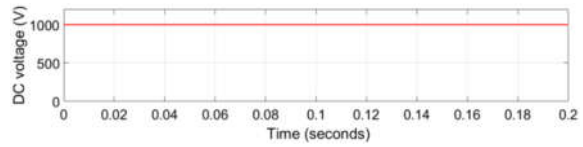

Figure 6. DC link voltage (stable at 1000V)

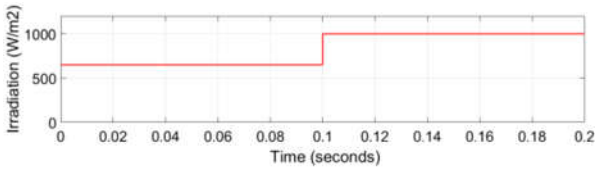

Figure 7. Solar irradiation step change at 0.1 second

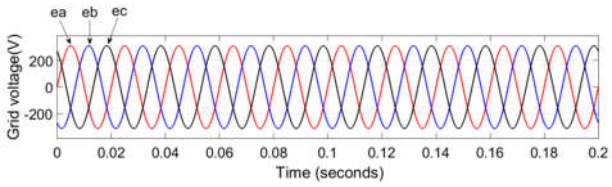

Figure 8. Grid voltages

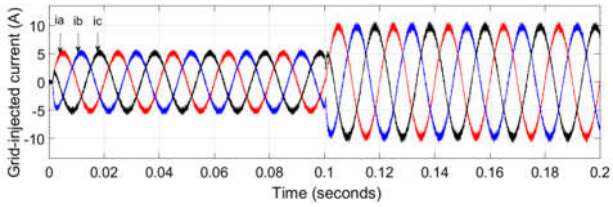

Figure 9. Grid-connected currents

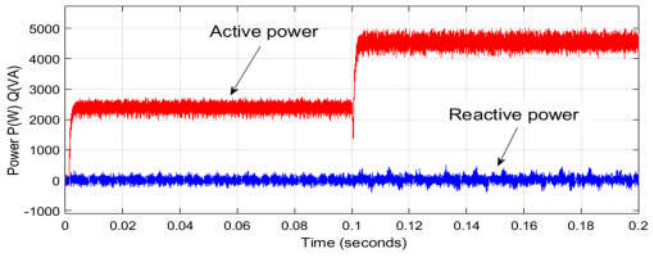

Figure 10. Output powers of the inverter

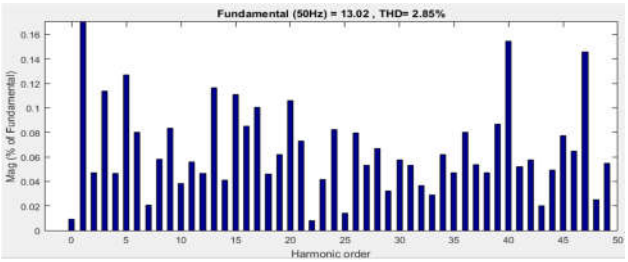

Figure 11. Harmonic analysis diagram of the grid-connected current corresponding to the irradiation of 650(W/m^2)

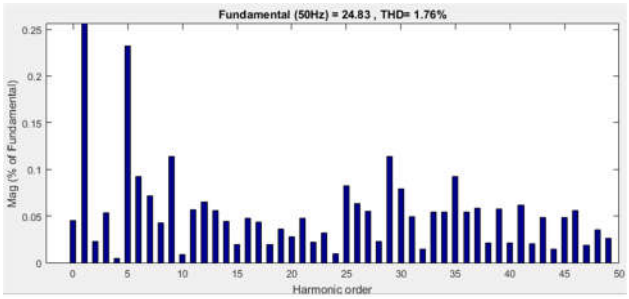

Figure 12. Harmonic analysis diagram of the grid-connected current corresponding to the irradiation of 1000(W/m^2)

6. CONCLUSION

This research successfully demonstrates the use of MPC in controlling the grid-connected current of the three-phase inverter for a PV system. This control method can maximize the active power and minimize the reactive power injected into the grid. In particular, the active power can quickly change according to the solar irradiation and the reactive power is approximately equal to zero. Moreover, the grid-connected currents always have THDs less than 5%, which are suitable with the required IEEE standard.

REFERENCES

[1]. Thuong Truong Quoc, Quyen Ngo Van, Son Nguyen Thanh, Cong Nguyen The, 2014. *Implementation of the controllers for maximum power point tracking of solar panel using LabVIEW*. Journal of Science and Technology, Technical Universities, Vietnam, September.

[2]. J. Rodriguez, P. Cortes, 2012. *Predictive control of power converters and electrical drives.* John Wiley & Sons.

[3]. Patricio Cortés, Gabriel Ortiz, Juan I. Yuz, José Rodríguez, Sergio Vazquez, Leopoldo G. Franquelo, 2009. *Model Predictive Control of an Inverter with Output LC Filter for UPS Applications*. IEEE Transactions on Industrial Electronics, Vol. 56, No. 6, pp. 1875-1883.

[4]. S. Kouro, P. Cortés, R. Vargas, U. Ammann, J. Rodríguez, 2009. *Model Predictive Control - A Simple and Powerful Method to Control Power Converters*. IEEE Transactions on Industrial Electronics, Vol. 56, No. 6, pp. 1826-1838.

[5]. P. Cortés, M. Kazmierkowski, R. Kennel, D. Quevedo, J. Rodríguez, 2008. *Predictive control in power electronics and drives*. IEEE Transactions on Industrial Electronics, Vol. 55, No. 12, pp. 4312-4324.

[6]. Joanie M. C. Geldenhuys, Hendrik du Toit Mouton, Arnold Rix, Tobias Geyer, 2016. *Model predictive current control of a grid connected converter with LCL-filter*. IEEE 17th Workshop on Control and Modeling for Power Electronics (COMPEL).

[7]. O. Matiushkin, O. Husev, D. Vinnikov, C. Roncero-Clemente, 2019. *Model Predictive Control for Buck-Boost Inverter Based on Unfolding Circuit.* Electrical and Computer Engineering (UKRCON) 2019 IEEE 2nd Ukraine Conference on, pp. 431-436.

THÔNG TIN TÁC GIẢ

Nguyễn Thanh Sơn[1], Phạm Hùng Phi[1], Nguyễn Thế Công[1], Lê Anh Tuấn[2], Phạm Văn Tuấn[3]

[1]Viện Điện, Trường Đại học Bách khoa Hà Nội

[2]Khoa Điện, Trường Đại học Công nghiệp Hà Nội

[2]Khoa Điện, Trường Đại học Sư phạm Kỹ thuật Vinh